JOURNAL OF THE AMERICAN WATER RESOURCES ASSOCIATION

AMERICAN WATER RESOURCES ASSOCIATION

The Hydrological Urban Heat Island: Determinants of Acute and Chronic Heat Stress in Urban Streams

Einara Zahn, Claire Welty, James A. Smith, Stanley J. Kemp, Mary-Lynn Baeck, and Elie Bou-Zeid

Research Impact Statement: Urbanization increases baseflow stream temperature and exacerbates stream temperature surges, creating a hydrological urban heat island.

ABSTRACT: During and after rainfall events, the interaction of precipitation with hot urban pavements leads to hot runoff, and its merger with urban streams can result in an abrupt change in water temperature that can harm aquatic ecosystems. To understand this phenomenon and its relation to land cover and hydrometeorological parameters, we analyzed data spanning two years from 100 sites in the eastern United States. To identify surges, we first isolated temperature jumps of at least 0.5°C over 15 min occurring simultaneously with water flow increase. Surge magnitude was defined as the difference between peak stream temperature and baseflow temperature right before the jump. At least 10 surges were observed in 53 of the studied streams, with some surges exceeding 10°C. Our results demonstrate that the watershed developed area and vegetation fraction are the best descriptors of surge frequency (Spearman correlation of 0.76 and 0.77, respectively). On the other hand, for surge magnitude and peak temperature, the primary drivers are stream discharge and stream temperature immediately before the surge. In general, the more urbanized streams were found to be already warmer than their more "vegetated" counterparts during baseflow conditions, and were also the most affected by temperature surges. Together, these findings suggest the existence of a hydrological urban heat island, here defined as the increase in stream temperature (chronic and/or acute), caused by increased urbanization.

(KEYWORDS: temperature; urbanization; runoff; thermal pollution; urban pavements.)

INTRODUCTION

It is well known that urbanization has the potential to alter the microclimate of cities (Santamouris 2011; Li and Bou-Zeid 2013; Mohajerani and Bakaric 2017). This is a result of a wide range of modifications to the land surface and surroundings, such as reduction of natural shading and evaporative cooling provided by vegetation (Li and Bou-Zeid 2013; Manoli et al. 2019), increased anthropogenic heat release (Sailor et al. 2015; Yang and Bou-Zeid 2018), and the preponderance of impervious and dark surfaces (Janke et al. 2009; Li et al. 2013; Ramamurthy et al. 2014; Mohajerani et al. 2017). This phenomenon, known as urban heat island (UHI), is characterized by the development of noticeably higher air and surface temperatures in cities compared with the countryside that directly surrounds them (Oke 1982, 1995; Mohajerani et al. 2017; Oke et al. 2017). According to a compilation of studies by Santamouris (2011), the UHI effect can boost air temperature in a city by as much as 15°C, and the differences are even larger for surface temperatures (Oke et al. 2017).

Paper No. JAWR-20-0125-P of the *Journal of the American Water Resources Association* (JAWR). Received September 5, 2020; accepted October 13, 2021. **Discussions are open until six months from issue publication**.

Department of Civil and Environmental Engineering (Zahn, Smith, Baeck, Bou-Zeid), Princeton University Princeton, New Jersey, USA; Department of Chemical, Biochemical and Environmental Engineering and Center for Urban Environmental Research and Education (Welty), University of Maryland, Baltimore County Baltimore, Maryland, USA; and Division of Science, Information Arts and Technology (Kemp), University of Baltimore Baltimore, Maryland, USA (Correspondence to Bou-Zeid: ebouzeid@princeton.edu).

Citation: Zahn, E., C. Welty, J.A. Smith, S.J. Kemp, M.-L. Baeck, and E. Bou-Zeid. 2021. "The Hydrological Urban Heat Island: Determinants of Acute and Chronic Heat Stress in Urban Streams." *Journal of the American Water Resources Association* 1–15. https://doi.org/10.1111/1752-1688.12963.

More recently, the existence of a subsurface UHI has also become well documented (Menberg et al. 2013; Westaway and Younger 2016). As explained in Oke et al. (2017), each UHI responds to different sets of scales and is caused by a different mix of processes, requiring distinct monitoring, and modeling schemes. However, the root cause remains land use modification associated with urban development.

The associated and concomitant impact of urbanization on the thermal state of the hydrosphere and water quality in streams, however, remains less studied than its surface and atmospheric counterparts. Some studies have addressed this question (LeBlanc and Brown 1997; Booth and Kraseski 2014; Hofmeister and Cianfrani 2015; Sun et al. 2015), showing the potential warming of streams and rivers (Pluhowski 1970; Rice and Anderson 2011; Somers et al. 2013; Fanelli and Prestegaard 2019; Ketabchy et al. 2019; Reza and Endreny 2019, 2020) and ponds (Brans et al. 2018) as a direct consequence of land use modification in urban watersheds. Surface-water warming evidence also has been analyzed at larger scales, as in some studies that documented increasing temperatures in the Chesapeake Bay (Ding and Elmore 2015; Rice and Jastram 2015). The links to the various UHIs would seem obvious, but have not been emphasized in previous studies. This paper aims to extend the UHI concept to include the impact of city development on the hydrosphere. To this end, we examine episodic (acute) and persistent (chronic) increments in urban stream temperatures compared to streams located in less disturbed environment surroundings to define a hydrological urban heat island (HUHI).

This thermal pollution is a result of several, often interacting local and watershed scale perturbations, including hydrologic connections to impervious surfaces, increased exposure to solar radiation caused by decreased riparian canopy cover, decreased forested area in the watershed, and direct inputs of warm water from power plant effluents and stormwater infrastructure (Somers et al. 2013; Iezzi and Todisco 2015; Ketabchy et al. 2019; Reza et al. 2020). Given that temperature is a primary indicator of the physical, chemical, and biological health of aquatic ecosystems (Sun et al. 2015), it is essential to understand how this parameter responds to disturbances, and which ones are most influential, in order to better quantify and mitigate possible negative impacts on biota. For instance, water temperature directly influences distribution, predator–prey interactions, survival, growth rates, timing of life-history events, and metabolism of aquatic organisms in river systems (Hannah and Garner 2015).

Of particular importance in recent studies is the acute response of stream temperature to rainfall events (Nelson and Palmer 2007; Rossi and Hari 2007; Anderson and Storniolo 2011; Rice et al. 2011; Somers et al. 2013, 2016; Zeiger and Hubbart 2015; Hathaway et al. 2016). In urban watersheds, the increase in the impervious fraction of the basin's surface area leads to an increase in runoff volume, faster response times, and higher peak discharge values (Leopold 1968). Given increased heat absorption, storage, and transfer capacity of paved surfaces, the interaction of rainwater with the heated ground leads to hot runoff that can rapidly drain to receiving water bodies, resulting in stream temperature surges (Gu et al. 2015; Omidvar et al. 2018; Omidvar and Bou-Zeid 2019). As an example, temperature increases of up to 11.2°C were observed in a pond receiving runoff from a parking lot in the Virginia Tech campus in Blacksburg, Virginia (Hester and Bauman 2013).

One of the first studies characterizing temperature surges in urban streams (Nelson and Palmer 2007) indicated that, after rainfall events, stream temperature increased on average by about 3.7°C, receding back to baseline over a period of 2.8 h. In addition, the most developed basin (urban land cover fraction of 90%) in that study registered temperature surges as high as 7.4°C. On the other hand, watersheds classified as agricultural did not have such abrupt changes in temperature, corroborating the idea that urbanization, and specifically heated impervious surfaces, play an important role in generating thermal loads to streams. Following this study, similar results were found for other urban streams and ponds (Anderson et al. 2011; Rice et al. 2011; Hester and Bauman 2013; Somers et al. 2013; Zeiger and Hubbart 2015; Croghan et al. 2019), where mean temperature surges between 2.4°C and 2.8°C were observed.

Development in the watershed and the fraction of impervious surface area are often pointed out as the best predictors for surge frequency. Nevertheless, some results (Nelson and Palmer 2007) show that local reach-scale land cover — such as deforestation in a 50-m zone around the stream — can be more important in dictating the number of temperature surges than the same index for the entire watershed. On the other hand, it remains unclear which land use characteristics modulate the intensity or magnitude of these higher temperature surges following rainfall events. While there is consensus that urban development in the watershed is a necessary condition for hot runoff flowing to the water body, it is not the sole component explaining surge magnitude. For instance, Somers et al. (2013) found that the highest temperature surges occurred in well-shaded streams as a consequence of the contrast between the cooler baseline temperature and the heated runoff. In addition, some results suggest an increasing trend in the frequency and magnitude of temperature surges in smaller drainage basins (Nelson and Palmer 2007).

Another feature suggested as playing a role is the distance between impervious surfaces and the receiving water body (Baruch et al. 2018), which is reflected in the land cover in a buffer around the stream (Rice et al. 2011), as well as how connected impervious surfaces are to the outlet.

The apparent discrepancies in the conclusions of some of these previous studies, and their use of different land use characteristics, make a meta-analysis challenging. The present study analyzes 100 stream gages in watersheds in the eastern United States (U.S.) that span the full continuum of urban development fractions (46 of which have an imperviousness fraction ≥20%), and relies on publicly available datasets, to compute consistent land use characteristics and provide a comprehensive assessment of how they influence stream water temperatures.

In addition to land-surface properties, hydrometeorological drivers — linking water balance and energy fluxes at surface-atmosphere interface — are important factors dictating thermal load to streams. This is documented in many studies aiming to model runoff temperature (Herb et al. 2008, 2009; Thompson et al. 2008; Janke et al. 2009; Omidvar et al. 2018; Omidvar and Bou-Zeid 2019). It is also corroborated by experimental studies linking surges to the thermodynamic and hydrological state of the air and water before the surge. For instance, some authors found air temperature (Picksley and Deletic 1999; Somers et al. 2016) to be an important driver of surge magnitude, while others (Nelson and Palmer 2007; Somers et al. 2016) investigated the role of average stream discharge on surge frequency. We extend these analyses in this paper to investigate a wide array of commonly measured hydrometeorological descriptors that are expected to affect surge frequency and magnitude. Some, like stream and air temperatures and baseflow discharge, have been examined before, while others, such as satellite-derived land-surface temperature are being investigated for the first time.

While others land use or hydrometeorological drivers of stream warming might exist, this study aims to focus on easily available "inputs" that can be readily computed by water managers to assess the risk of elevated stream temperature. They can also be used by other investigators in future studies at different sites, which would facilitate meta-analyses. For example, we represent urbanization for all watersheds by indices derived from one and land cover dataset, which is freely available to the community. In addition, the large number of streams here investigated covers a broad range of land use and hydrometeorological conditions. This diversity provides the opportunity to assess the generality of the mechanisms and watershed characteristics that exacerbate thermal pollution, with the aim of obtaining more conclusive evidence of the connection between surges and land use.

The overarching goal of this work is thus to compare the frequency and intensity of stream temperature surges across many watersheds and to identify the main physical drivers of this phenomenon. To that end, we ask the following questions: Which land surface characteristics are the best descriptors of the number and magnitude of the surges? Are surge characteristics influenced by antecedent hydrometeorological conditions? What dictates the overall thermal stress in urban streams? This last question entails whether the temperature extremes caused by surges are larger than the maximum values observed over a typical diurnal cycle without the occurrence of surge, and documents baseflow stream temperature dependence on urban development.

Overall, our results elucidate the role of developed areas in exacerbating the frequency of temperature surges, as well as in increasing the baseflow water temperature. Streams in highly developed watersheds are warmer than their "vegetated" counterparts (less developed watersheds) both at long time scales (chronic effect) and during shorter episodes of acute temperature surges. These confirm the existence of a HUHI, defined as the increase in urban stream temperature compared to their countryside counterparts.

MATERIALS AND METHODS

Data

We conducted a survey of all stream gages having co-located stream temperature observations (T_S) maintained by the U.S. Geological Survey (USGS), retaining those that met the following criteria: temporal resolution of 15 min or shorter; observations for at least spring and summer of 2017 and 2018; and availability of discharge or gage height time series during the same period. To represent different watershed sizes, from this group we further selected gages with contributing drainage areas ranging from 0.26 to 89 km^2. In addition, temperature observations at five USGS stream gaging stations located in Baltimore, collected by the University of Maryland, Baltimore County (Welty and Kemper 2019), were added to our dataset.

Ideally, all regions of the country would be represented; however, the lack of USGS gages in some states, the failure to meet some of our criteria, or the presence of stream discharge control caused by dams, precluded a broader geographic representation. Nonetheless, we were able to retain data from 100 gages across 19 states, with the broad spatial distribution and climatic characteristics as shown in Figure 1 (a detailed description of the stream gages is compiled in Table S1). Half of the gages are located in the states of Maryland, Georgia, and Kentucky. Regarding climatic zones (Peel and Finlayson 2007), 23 gages are characterized as *Dfb* (cold, no dry season, warm summer), 13 as *Dfa* (cold, no dry season, hot summer), and 63 as *Cfa* (temperate, no dry season, hot summer). One additional gage not shown in the figure is located in the state of Washington and characterized as *Csb* (temperate, dry, and warm summer). We note that the climatic zone classification shown in Figure 1 is for reference only. In our analyses, we do not attempt to link surge frequency or magnitude to mean climatic conditions, but rather to the hydrometeorological conditions preceding the storms.

All stream temperature and discharge data were downloaded from the USGS website using the R package dataRetrieval (Hirsch and De Cicco 2015). Furthermore, shapefiles for all watersheds (area draining to the respective gage locations) were obtained through the StreamStats USGS application (Accessed June 2020, https://streamstats.usgs.gov/ss/). For the land cover characterization, we used the National Land Cover Database (NLCD) 2016 (Homer et al. 2020) products for land cover and imperviousness (Yang et al. 2003). All raster manipulations were conducted using the software ArcGIS (https://www.arcgis.com) in conjunction with the python package ArcPy (https://www.esri.com/en-us/arcgis/products/arcgis-python-libraries/overview), facilitating the implementation of the ArcGIS geoprocessing tools over many datasets. To this end, the ArcPy functions "Clip" and "BuildRasterAttributeTable" were used to extract indices for each watershed. In addition, the Arcpy function "Buffer" was used to create circular buffer zones with radii of 200 or 400 m around each stream gage, for which the same land cover indices (listed below) were also extracted. The aim was to investigate whether the characteristics of these smaller buffer zones that focus more on the riparian zones around the stream gage are better at explaining the temperature surges than the characteristics of the whole watershed.

The following indices were computed for each basin: percent developed, here defined as the sum of low, medium, and high intensity developed areas (indices 22, 23, and 24 of the NLCD classification); percent forest (indices 41–43); percent shrubs (51 and 52); percent grass, herbaceous, lichens, and moss (71–74); and percent pasture/crops (indices 81 and 82). Across all vegetation categories, forests were the most

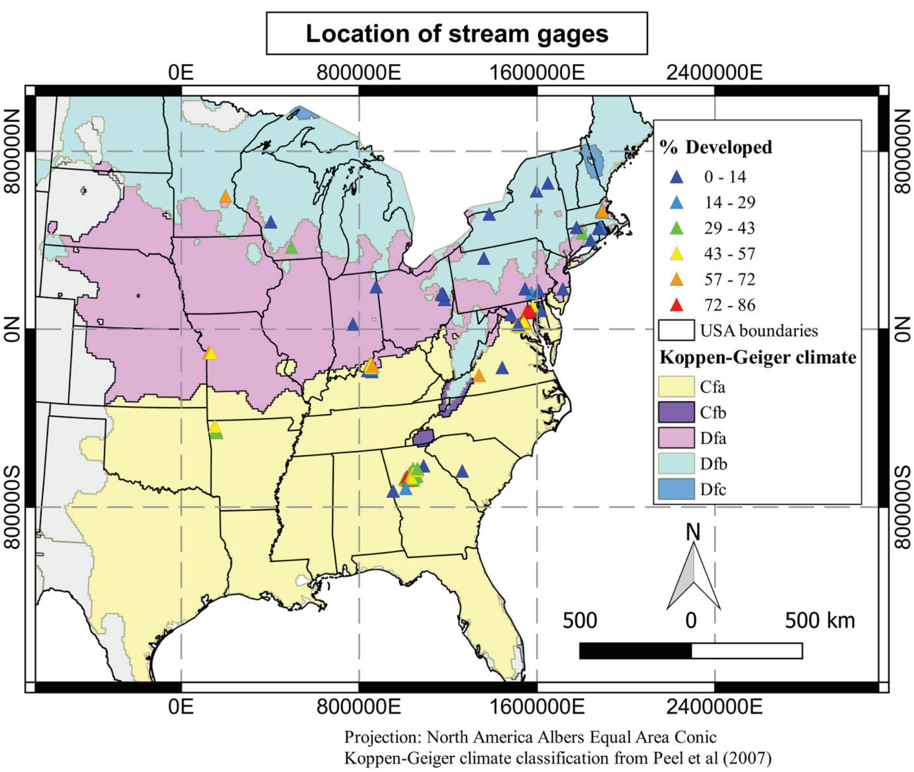

FIGURE 1. Location of United States Geological Survey stream gages and their respective climate zones as given by the Köppen–Geiger classification. Climatic zones based on dataset of Peel et al. (2007). Note that we also use data from one stream in the state of Washington.

predominant, followed by pasture and crops. These "green" indices were combined into a single index called vegetation. This index represents the proportion of the watershed that is covered by any type of vegetation (natural or agriculture), representing soil with larger permeability than regions with built surfaces, such as roads or compacted urban soils. In our analyses, this index (including all vegetation categories) was better correlated (Spearman correlation $r = -0.76$, $p < 0.05$) to the frequency of surges than if only individual categories were included (Spearman correlation $|r| < 0.68$ and $p < 0.05$, for individual vegetation categories such as only forests), reflecting the fact that all vegetated surfaces will lead to less frequent temperature surges and cooler runoff.Supporting Informationcontains figures summarizing the individual contributions of each type of vegetation, as well as the proportion of the watersheds classified as low, medium, and highly developed. Similarly to vegetation, we also confirmed that the total percent developed area resulted in a better correlation with surge frequency than any of its individual components.

Additionally, we computed the percent impervious land cover from the NLCD urban imperviousness product, which represents the percentage of impervious cover over each 30-m pixel. Based on the imperviousness fraction of each 30-m pixel, we then computed the total impervious area in the watershed. Note that this index is different from and smaller than the index representing the developed area, the latter including impervious surfaces as well as "developed" vegetated surfaces such as urban lawns. The index for development simply lumps all pixels classified as low, medium, or highly developed, and does not exclude the presence of open lands such as grass fields in backyards, parks, or empty lots. As an example, a pixel categorized by the NLCD as medium development is expected to have an imperviousness in the range 50%–79%; the remainder of this pixel is included in the developed index, but not in the impervious index. Therefore, while percent imperviousness and percent developed are positively well correlated, and can both serve as indicators of urbanization, they are different descriptors of urbanization and both were tested and contrasted to previous studies that examined them. Throughout the text, we refer to the indices percent developed and percent impervious when discussing the results of the statistical analyses. Nonetheless, we also refer to the broad qualitative terms "urban" and "urbanized" in the general context when referring to areas where land cover was modified by the human presence, usually resulting in an increase in percent developed and imperviousness.

Additional data used in our analysis were land surface temperature (T_L) and air temperature (T_A). Surface temperature at 30-m resolution (Cook et al. 2014) was obtained from the U.S. Landsat Analysis Ready Data (Egorov et al. 2019) through USGS Earth Explorer. Although only available every 16 days for each region, T_L on selected sunny days (cloud cover <10%) during summer were used to characterize the thermal properties of the watershed surfaces and their propensity to heat up before rainfall (more details about temperature surge descriptors are given below). Finally, air temperature and relative humidity, both later used to compute the wet-bulb temperature (Stull 2011), for each gage were obtained from the closest station of the Automated Surface Observing System (Accessed July 2020, https://www.ncdc.noaa.gov/data-access/land-based-station-data/land-based-datasets/automated-surface-observing-system-asos).

Temperature Surge Metrics and Descriptors

The most common definition of temperature surge in the literature is a temperature increase above a specified threshold in a stipulated time period. For instance, Nelson and Palmer (2007) defined a temperature surge as a temperature jump >2°C during a time period of 30 min. Reflecting the availability of higher temporal-resolution time series, other authors have defined temperature surge as a jump >1.0°C in 10 or 15 min (Anderson et al. 2011; Rice et al. 2011; Somers et al. 2013; Zeiger and Hubbart 2015). As a proxy for runoff input, simultaneous precipitation (Croghan et al. 2019), increase in discharge flow (Nelson and Palmer 2007), or stage (Hester and Bauman 2013) are usually used.

With the exception of stream temperature measurements in Maryland and District of Columbia (which have time resolution as high as one minute), temporal resolutions between 5 and 15 min are more common. Consequently, we chose 15 min as our window to investigate abrupt changes in temperature. Furthermore, in order to have a general picture of the most probable temperature surge increase after rainfall events, we defined a temperature surge as a jump equal to or >0.5°C. For each detected surge, we matched the temperature time series with discharge (91 gages) or gage height (9 gages) to verify that there was a simultaneous increase in streamflow. Because surges are more common during warmer months, we only considered days from mid-April to mid-October (generally having T_S >10°C).

To represent surge frequency, we calculated the fraction of days with surges, given by the ratio of days with at least one surge by the total number of investigated days. For intensity, we defined two indicators for the maximum and the mean. The maximum temperature reached during an event was defined as $T_{S,peak}$, after which the stream water started cooling off toward the equilibrium value as the runoff input ceased. The magnitude of the temperature surge can then be calculated as the difference between the temperature peak and the baseline temperature:

$$\Delta T_S = T_{S,peak} - T_{S,0}, \quad (1)$$

where $T_{S,0}$ is the temperature before the surge (in this paper, the subscript "0" always denotes baseline conditions, corresponding to the state immediately before the surge). We defined $T_{S,0}$ as the temperature at the start of a 15-min moving window during which a surge ≥0.5°C was detectable. In addition, we encountered many cases with multiple surges occurring during the same rainfall event; for these cases, we computed ΔT_S for each peak, where $T_{S,0}$ was derived from the decreasing limb of the previous surge (effectively it would be the temperature minimum between the surges). These composite surges led to smaller surge magnitudes for the second peak onward. Following Picksley and Deletic (1999), we also computed the event mean temperature (EMT), defined as

$$\text{EMT} = \frac{\int_0^{t_{peak}} \Delta Q \Delta T_S dt}{\int_0^{t_{peak}} \Delta Q dt}, \quad (2)$$

where $\Delta Q = Q - Q_0$ is the stream discharge minus the baseline value and t_{peak} is the time when the stream temperature reaches its peak. This time interval was chosen because of the uncertainty in automatically detecting the end of each temperature surge, which in many cases did not show a decrease toward the baseline value or were followed by another jump ≥0.5°C. The EMT indicator quantifies the integrated excess advective heat flux normalized by the integrated excess mass flux, and thus represents the surge mean intensity.

Tested descriptors based on land surface characteristics are % developed land area, % vegetation, % impervious, and drainage area. To represent the temperature gradient between land surface and water, we defined the overheating index $\text{OHT} = \hat{T}_L - \tilde{T}_S$, where $\hat{T}_L$ is the spatial average (denoted by the circumflex, over each watershed) of the land surface temperature and $\tilde{T}_S$ is the time average of the stream temperature over the acquisition day of the satellite images used to derive T_L. Hydrometeorological descriptors were mean baseline stream $\bar{T}_{S,0}$ and air $\bar{T}_{A,0}$ temperatures, and baseline discharge $\bar{Q}_0$ (for gages with discharge data available). Here the overbar denotes the average over all surge events for each gage (for instance, $\bar{Q}_0$ is the average of Q_0 for all surges at the same gage). To improve the statistical representativeness of the observed surges, these averages were only computed for a stream that registered at least 10 surges in the two analyzed years (2017 and 2018). Therefore, analyses involving predictors of mean surge magnitude only consider streams with at least 10 surges. On the other hand, all streams are included when predictors for surge frequency are investigated.

To test the best determinants for both surge frequency and magnitude, we used the nonparametric Spearman correlation coefficient *r*, chosen given the nonlinearity between most pairs of variables. This way, we can find the best-correlated variables without a priori defining the "shape" of their relation. In addition, we compute the Pearson correlation coefficient (r_p) for some of our analysis (when linearity was observed).

Finally, to investigate the baseflow stream temperature, we isolated all days that did not register any temperature surge, considering these days as "undisturbed" (as opposed to "disturbed" by the input of hot runoff in days with surges). We then computed the peak daily stream temperature considering only undisturbed days. These values were later contrasted to maximum temperatures achieved during a surge, indicating those streams where extreme temperatures were exacerbated because of the input of hot runoff.

RESULTS AND DISCUSSION

Temperature Surge Statistics

Evaluating the entire record for all gages, 2,261 surges were identified. From the set of 100 investigated streams, 53 registered at least 10 surges in the two analyzed years, the most extreme case being 155 surges (covering 27% of the total number of days).

Nearly 69% of the surges were ≥1.0°C, whereas 28% were ≥2.0°C. Furthermore, a smaller proportion (≈3.4%, 77 surges) were in the range 5.0°C–10.3°C, found more often in the most developed watersheds (Figure 2). Maximum temperature increases in this range were also reported in other urban streams by previous studies (Nelson and Palmer 2007 [7.4°C]; Hester and Bauman 2013 [8.1°C]). The temporal distribution of ΔT has a similar behavior to the results found by Hester and Bauman (2013). Temperature surges were more frequent in the afternoon, with a

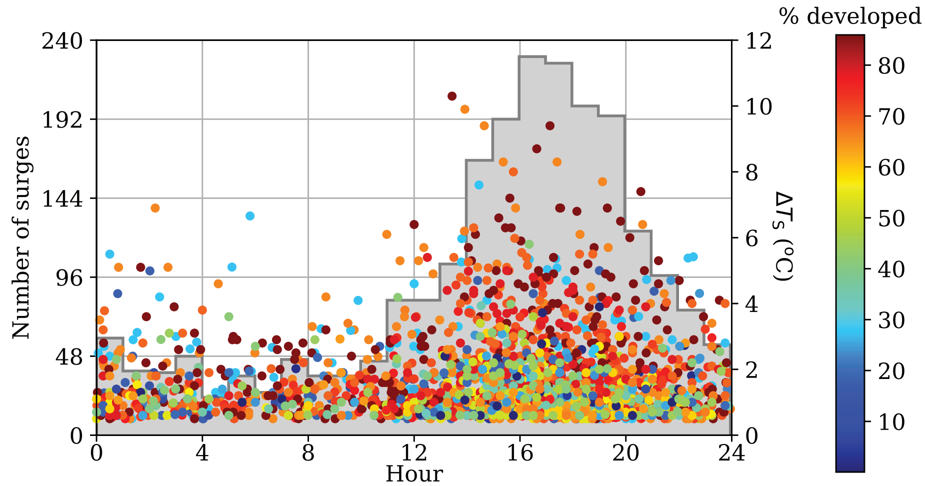

FIGURE 2. Histogram (gray) of the number of surges per hour (standard local time) and scatter plot of surge magnitude ΔT_S (n = 2,261). The time refers to the moment a first jump ≥ 0.5°C was detected. Colors represent the % developed land area in each watershed.

peak around 16:00 (approximately 76% occurred between noon and midnight). Furthermore, increases >6.0°C were almost entirely restricted to the period between noon and 20:00. These results show a general picture in which rainfall events in the afternoon — when the land surface is hot due to intense and prolonged insolation — lead to a runoff with a higher temperature than the receiving stream. In addition, despite the hottest surges being registered during daylight hours, surges as high as 7.6°C were observed between midnight and 06:00, illustrating the potential of these pavements to remain hotter than their surroundings hours even after sunset.

Influence of Land Cover on Surge Frequency

The results in Figure 2 suggest a strong linkage between thermal pollution and urbanization of land cover; this is not a new result, as this has been found in other streams in Maryland and North Carolina (Nelson and Palmer 2007; Somers et al. 2013). However, our larger sample size allows us to probe the correlation between surge intensity and frequency with land cover and watershed characteristics (at the catchment scale) with a more robust dataset than previous studies. Thus, we can investigate gages with various degrees of development (as a continuum), rather than the two extremes only (low and high development).

The scatter plot of the number of days with surges vs. area and land surface descriptors confirms the strong connection between surge frequency and the degree of development in the watershed (Figure 3b), also reflected in the % of vegetation (Figure 3a). For instance, gages in watersheds covered by >60% vegetation experience <3% of days with surges. In these watersheds, the large area occupied by vegetation reduces the soil temperature and increases the permeability, reducing the runoff temperature by both decreasing heat advection and delaying its generation. On the other hand, streams that exhibited surges in more than 10% of days were located primarily in watersheds that are more than 60% developed. The converse, however, is not true: Some urban streams registered few surges. Development is thus a necessary but insufficient condition for a high frequency of surges.

The Spearman correlation coefficient (Table 1) confirms these results: percent developed and percent vegetation are the best determinants for the number of surges (Spearman correlation coefficient equal 0.76 and −0.77, respectively). We also tested percent impervious fraction as a descriptor of surge frequency, but it showed similar results to the developed fraction as both indices are well correlated (figure not shown here). This is in contrast to the results found by Nelson and Palmer (2007), who found imperviousness (Pearson $r_p = 0.69$) to be a better explanatory variable than percent urban (r_p = 0.42), which they defined in a similar way to our percent developed (but with a different land cover dataset). They also found a positive correlation between percent deforestation and surge frequency ($r_p = 0.60$). However, our sample size is larger (100 watersheds as opposed to 16), which gives us confidence that our correlations and conclusions are robust. In this regard, our dataset (the NLCD database) and the modified land surface explanatory variables (for instance, % vegetation instead of only % forests) seem to be more adequate to explain surge frequency.

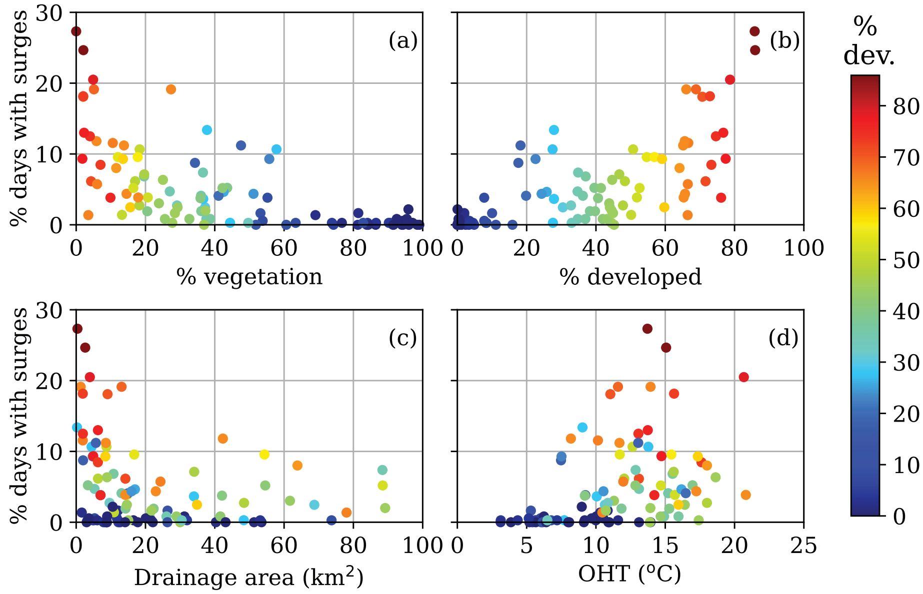

FIGURE 3. Plot of % of days with surges vs. (a) % vegetation, (b) % developed fraction, (c) drainage area, and (d) overheating of the subwatershed (OHT) (see text for definition). In all plots, the colors represent the % developed fraction in the respective watershed.

Nelson and Palmer (2007) also found that deforestation in a buffer around the stream (50 m on each side) was a better predictor ($r_p = 0.76$) than considering the same index for the entire watershed. In our analyses, we thus tested all land surface descriptors on a buffer around the gage (200 and 400 m); however, the correlations were similar or inferior to those obtained for the whole subwatershed and are not shown here.

Figure 3c and 3d show the relation of surge frequency with drainage area and OHT, respectively. The first shows a negative correlation (Spearman correlation coefficient equal −0.30, $p < 0.05$; Table 1), with smaller watersheds registering more surges. For instance, watersheds smaller than 20 km^2 and a developed fraction larger than 60% resulted in surges in at least 15% of the days. The overheating index OHT, on the other hand, shows a positive correlation (Spearman $r = 0.52$, $p < 0.05$). All watersheds with surge frequency >15% had an OHT larger than 10°C, meaning that the land surface in these watersheds is at least 10°C hotter than the stream on a typical sunny summer day. However, there are gages with large OHT but few or no surges, as can be seen for less developed watersheds (developed fraction <20%). This is an interesting and new result since it indicates that natural surfaces, even when they can display large overheating relative to the stream, do not generate temperature surges due to larger infiltration, and more storage in topographic depressions, resulting in a lower and slower runoff. Again, the presence of an envelope curve for this explanatory variable indicates the interaction of many variables in dictating temperature surges.

TABLE 1. Spearman correlation coefficient of % of days with surges, 90th percentile of event mean temperature (EMT), and average of stream temperature peak vs. land surface descriptors (% vegetation, % developed, drainage area) and watershed OHT.

	% of days with surges	EMT90%	$\bar{T}_{S,peak}$
% vegetation	−0.77*	−0.17	−0.28
% developed	0.76*	0.26*	0.24
Drainage area	−0.30*	−0.58*	0.45*
OHT	0.52*	0.01	0.31*

*p-values ≤0.05 indicating a 95% confidence that the trends are statistically significant.

We also computed overheating indices by subtracting the air and wet bulb temperature (as a proxy for rain temperature) from the land surface temperature, but they did not result in better correlations. In addition, other statistics were tested for both land surface and stream temperature, such as maximum and 90th percentile, but similar or inferior correlations were found, compared to the four leadings determinants in Figure 3, and the results are not shown.

The frequency of surges was also regressed against hydrometeorological determinants, including mean discharge ($\bar{Q}_0$) and mean air temperature ($\bar{T}_{A,0}$) immediately before the surge. However, with exception of $\bar{Q}_0$ — which is correlated with drainage area — these descriptors were found to be less important in explaining surge frequency than the land surface characteristics we depict in Figure 3.

Influence of Watershed Characteristics and Hydrometeorology on Surge Intensity

In this section we discuss the best determinants of EMT during a surge; specifically, the 90th percentile ($EMT_{90\%}$) of this indicator over all surges is investigated for each stream. We also tested the mean magnitude difference, ΔT_S, but it showed similar or slightly inferior results to EMT and is not shown.

Drainage area is the watershed characteristic that best explains $EMT_{90\%}$ (Spearman correlation of −0.58, $p < 0.05$; Table 1). This negative correlation of EMT with area is shown in Figure 4c. Surprisingly, despite percent development being highly correlated with surge frequency, it is not a very good descriptor of the intensity, as deduced from the EMT, during a surge event (Spearman correlation of 0.26, but statistically significant). Furthermore, the overheating index — which indicates the temperature contrast between land and water — also resulted in a smaller than expected correlation (Spearman $r = 0.01$, not statistically significant) with $EMT_{90\%}$. However, this correlation could be affected by the use of one land surface temperature image for each watershed taken on a sunny day, thus not showing the temporal variation of T_L or the conditions prevailing before rainfall that tend to be cloudy.

In addition to watershed characteristics, we investigated which hydrometeorological variables could best explain $EMT_{90\%}$. The mean baseline discharge (i.e., mean Q before surges) was the best hydrological explanatory variable for this surge intensity metric (Figures 4a), with a Spearman correlation of −0.63 ($p < 0.05$) shown in Table 2. The smaller the baseline flow, the larger the temperature change in the stream (larger $EMT_{90\%}$).

Looking at stream and air temperatures immediately before the surges, we found that the smaller these baseline values, the larger ΔT_S and consequently $EMT_{90\%}$ (Figure 4b). The negative correlation (Spearman correlation coefficient of −0.65, $p < 0.05$) between $EMT_{90\%}$ and $\bar{T}_{S,0}$ is an expected result — especially in smaller streams — which follows from the large temperature difference between the cooler baseline water body and the heated runoff water it is receiving. Large temperature surges occurring in cooler baseline temperatures can be seen in well-shaded streams, as pointed out by Somers et al. (2013), where riparian vegetation prevents part of the solar radiation from reaching the water. This occurs in some of the most urbanized watersheds investigated in this study (verified by visual inspection of pictures and satellite images for these sites), for instance, in Baltimore, Maryland, Washington, District of Columbia, and Atlanta, Georgia. Such streams were visually inspected to be surrounded by tall trees that likely intercept most of the solar radiation and help create an environment of cooler temperatures. Nonetheless, while these streams might be well shaded — keeping their water temperature cooler — their urban surroundings still transfer hot runoff to them, creating rapid temperature surges. The negative correlation between $EMT_{90\%}$ and $\bar{T}_{A,0}$ (Figure 4b) is likely indirectly related to the positive correlation between air and stream temperature.

Implications for Thermal Stress and Ecosystem Health in Urban Streams

In the previous section, we focused on the surge magnitude as an important indicator for increased thermal stress in urban streams. But given that the largest increases occurred in streams with cooler baselines, the third question we asked in the introduction "What dictates the overall thermal stress in urban streams?" remains open. Therefore, we now focus on the absolute temperatures recorded in streams during storms, as well as under baseline conditions.

For periods with surges, we investigate the maximum stream temperature after a surge, averaged over all surges for each stream ($\bar{T}_{S,peak}$). We regressed this statistic against the same watershed and hydrometeorological indicators considered in the previous subsection to explain EMT. Again, the drainage area was found to be the watershed characteristic that best explains $\bar{T}_{S,peak}$ (Spearman correlation of 0.45 and $p < 0.05$, Table 1; Figure 5c). A positive correlation was also noted between $\bar{T}_{S,peak}$ and baseline flows (Spearman correlation of 0.41 and $p < 0.05$, Table 2; Figure 5a). These two results are related since larger watersheds have larger baseline flows. Together, they confirm that the larger streams investigated in this study tend to have higher baseline temperatures (for a multitude of reasons including potentially lower shading); therefore, even though they need not have the larger surges (see previous subsection), they attain the highest peak temperatures.

We also tested the overheating index (OHT) as a descriptor of $T_{S,peak}$, but the results indicated a smaller than expected correlation ($r = 0.31$, $p < 0.05$). While development is not the best explanatory variable for extreme temperatures, it is worth observing that if one focuses on streams with small drainage area in Figure 5c, only the most developed streams tend to produce high peaks and those peaks are comparable to much larger, less developed watersheds. For instance, the average $T_{S,peak}$ in some of the smallest and most developed streams (percent developed ≈80%) reaches values around 25°C, which is

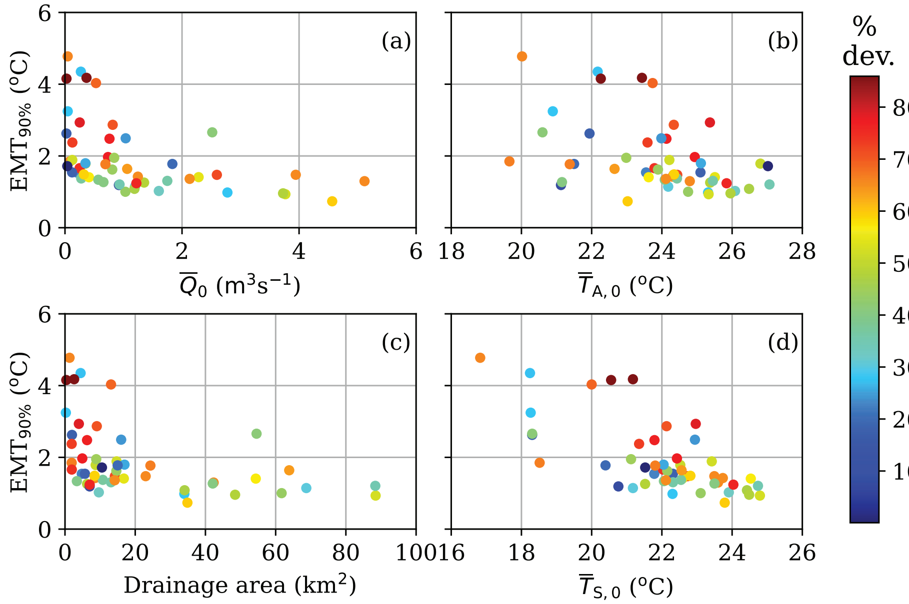

FIGURE 4. Plot of 90th percentile of EMT vs. (a) mean baseline discharge $\bar{Q}_0$, (b) mean baseline air temperature $\bar{T}_{A,0}$, (c) drainage area, and (d) mean baseline stream temperature $\bar{T}_{S,0}$, where baseline refers to the state immediately before surge.

TABLE 2. Spearman correlation coefficient of % of days with surges, 90th percentile of EMT, and average of stream temperature peak vs. mean baseline discharge ($\bar{Q}_0$), drainage area, mean baseline air temperature ($\bar{T}_{A,0}$), and mean baseline stream temperature ($\bar{T}_{S,0}$).

	% of days with surges	$EMT_{90\%}$	$\bar{T}_{S,peak}$
$\bar{Q}_0$	−0.56*	−0.63*	0.41*
Drainage area	−0.30*	−0.58*	0.45*
$\bar{T}_{A,0}$	−0.23	−0.48*	0.61*
$\bar{T}_{S,0}$	−0.32*	−0.65*	0.96*

*p-values ≤0.05 indicating a 95% confidence that the trends are statistically significant.

similar to the averages found in streams with a drainage area larger than 40 km^2 and percent developed 40%–50%.

The peak temperature $\bar{T}_{S,peak}$ also showed strong positive correlations with $\bar{T}_{A,0}$ ($r = 0.61$ and $p < 0.05$, Figure 5b) and $\bar{T}_{S,0}$ (0.96 and $p < 0.05$, Figure 5d). In this case, watersheds with high air or stream baseline temperatures also resulted in the highest temperature peaks after surges. Although this may seem like an obvious result, it highlights that streams that are already disturbed by urbanization — being hotter than "vegetated" streams — are further impacted by temperature surges. Nonetheless, note that the streams with the largest $\bar{T}_{S,peak}$ are not necessarily streams with a larger developed fraction (although still highly developed), and this is likely the result of the confounding effect of other factors, such as shading, that can reduce peak temperatures even in highly developed streams, as explained earlier.

So far, we have shown that temperature surges can increase stream temperature by up to 10.3°C and are more common in developed watersheds. However, the peak temperatures reached during these surges were also strongly modulated by the stream's baseline temperature that was affected by drainage area, shading, and factors not directly related to urbanization. One important remaining question is thus to what extent does urbanization alone modify the baseline temperature observed in these streams? That is, does urbanization increase baseline temperature as well as surges, thus creating a synergistic risk to stream health?

To answer this question, we plot the distributions of maximum daily stream temperature on undisturbed days (when no surge occurred) in Figure 6, where upper and lower whiskers represent maximum and minimum values and the size of the box corresponds to the interquartile range. Boxplots were ordered in the figure by percent developed area as indicated by the colorbar. Note that the x-axis represents the gage number (from 1 to 100), not percent developed. Figure 6 also shows $T_{S,peak}$ in gray markers (i.e., the maximum temperature achieved after all registered surges), which happened on "disturbed" days, but may or may not correspond to the maximum stream temperature observed on a respective day.

The average daily maximum T_S increases in a linear fashion with percent developed area in the watershed, resulting in a Pearson correlation coefficient $r_p = 0.44$ ($p << 0.01$; linear regression not

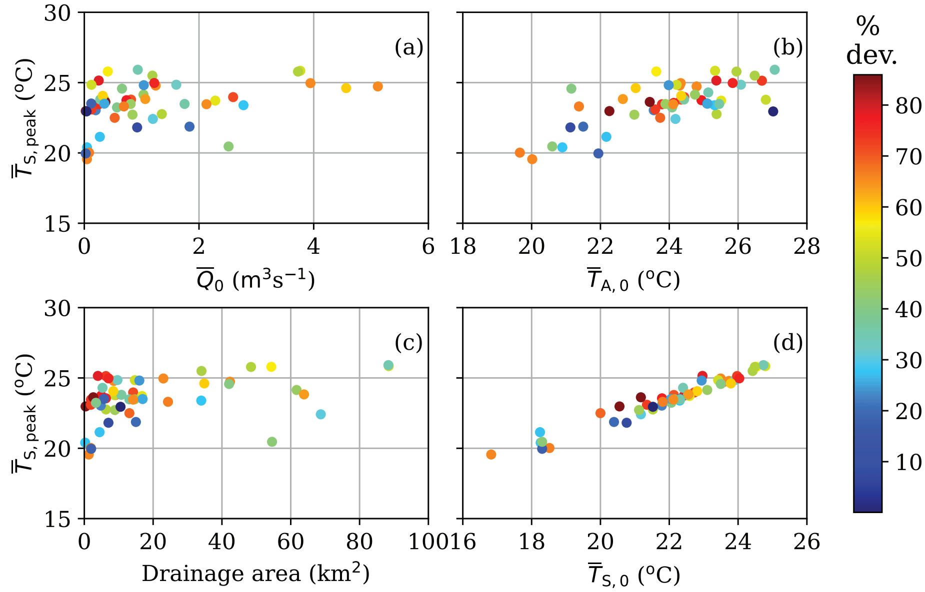

FIGURE 5. Plot of $\bar{T}_{S,peak}$ vs. (a) mean baseline discharge $\bar{Q}_0$, (b) mean baseline air temperature $\bar{T}_{A,0}$, (c) drainage area, and (d) mean baseline stream temperature $\bar{T}_{S,0}$, where baseline refers to the state immediately before surge.

shown). A similar correlation is obtained using the Spearman correlation coefficient (r = 0.45, p << 0.01). As shown in Figure 6, some of the most developed sites (developed area >70%) show a decline in T_S compared to less developed sites, which is likely caused by local factors as previously mentioned. Nonetheless, these results indicate that stream temperature on undisturbed days, which represents a "background" state, tends to be warmer in more developed basins as a result of other direct and indirect urbanization impacts (Rice et al. 2011; Rice and Jastram 2015). In addition, streams in more developed watersheds not only registered more surges, but also had more cases where the maximum temperature after a surge was larger than the maximum temperature on undisturbed days. For instance, the most developed watershed registered a temperature peak caused by a surge that was 4.0°C larger than the maximum value registered considering all undisturbed days. In addition, even when not larger than the baseline temperatures, $T_{S,peak}$ is usually in the upper range (between median and upper limit) of the distribution of maximum temperature on undisturbed days.

For streams with at least 10 surges, we also regressed the average daily maximum T_S against $\bar{T}_{S,peak}$, finding a positive linear correlation (r_p = 0.88, p << 0.01, figure not shown). Alternatively, we also computed the Spearman correlation coefficient (r = 0.82, p << 0.01). These results are similar to the ones reported in Figure 5d, but now using temperature on undisturbed days as a descriptor instead of baseline temperature immediately before surges. Both results concur that warmer streams are more impacted by temperature surges, resulting in even larger temperature extremes.

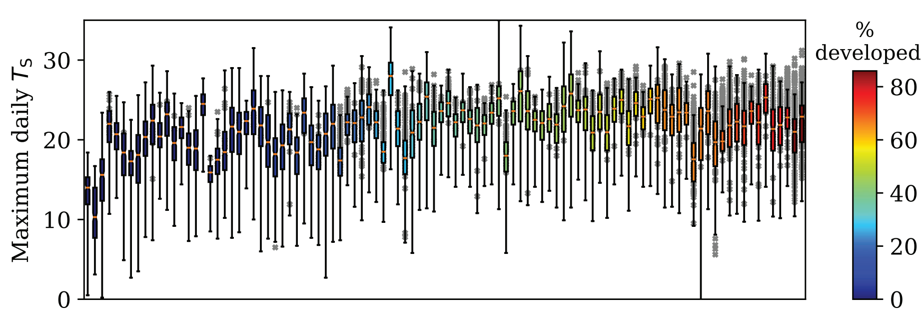

FIGURE 6. Boxplot of maximum daily stream temperature on undisturbed days (when no surge occurred) registered at each gage. Upper and lower whiskers are the maximum and minimum values, while the box size is the interquartile range. Gray markers are the temperature peak after all surges. Only days between April 15 and October 15 of 2017 and 2018 are included.

Our findings therefore indicate that urban streams are altered in two main ways: chronic — caused by long-term warming — and acute — caused by temperature surges. These results thus confirm the existence of a HUHI, which refers to an increase in the temperature of urban streams (and potentially other surface water bodies) compared to their vegetated counterparts. These impacts are directly linked to urban modifications in the environment surrounding such streams as our analysis confirms: if the same streams were located in undisturbed or less urbanized regions, baseline temperatures would be lower and runoff temperature surges would be less frequent.

The increase in the water temperature may increase the rates of microbial decomposition and primary production (Demars et al. 2011; Scrine et al. 2017), alter the rate of chemical reactions (Kaushal et al. 2018), and disturb ectothermic aquatic organisms (Scrine et al. 2017). Change in warming patterns may also lead to a change in aquatic communities: as species that are less adapted to warm waters tend to migrate to colder waters, warm-adapted and tolerant species can become dominant (Krause et al. 2004; Scrine et al. 2017).

An important aspect of life in aquatic ecosystems is that the thermal tolerance of organisms, such as fish, depends on the temperature of acclimation (Kowalski et al. 1978). In general, higher acclimation temperatures result in tolerances to higher temperatures (Kowalski et al. 1978; Beitinger and Bennett 2000). Seasonal changes in baseline water temperatures and subsequent acclimation to those temperatures provide fish with a larger thermal tolerance safety margin during warmer months (Beitinger and Bennett 2000). However, temperature surges caused by the input of hot runoff could result in temperature peaks that exceed seasonal thermal tolerances for some species. For instance, acclimation temperatures in spring months would be lower, and water temperature surges could increase water temperatures beyond acclimated thermal tolerances and cause thermal stress. As an example, Terpin and Spotila (1976) found that blacknose dace — a species commonly found in the eastern U.S., where most of the investigated streams are — have smaller chances to survive if, after acclimating to 20°C for a month, it is exposed to temperatures equal to or larger than 31°C for two hours. In more extreme cases, they found that 39 min of exposure to temperatures larger than 31.5°C was lethal.

Unfortunately, as highlighted by Kemp (2014), there is a lack of information regarding the thermal tolerance of species (especially nongame species and during sensitive life history stages) living in urban watersheds, which prevents a more detailed analysis of thermal impacts on the streams studied here. Nevertheless, this broad view already shows how thermal pollution can be detrimental to aquatic ecosystems. Note that these effects refer to water temperature increase alone; the risk is even more complex and acute when considering the plethora of other stressors, such as chemical pollution, also advected with the runoff (e.g., nutrients, bacteria, and oils from parking lots), flashy high peak flows (Walsh et al. 2005), as well the hydroclimatic shifts that can result from climate change such as reduced baseflow or increasing baseline temperatures. These stressors can combine with the HUHI to increase the environmental risks for ecosystems and their fauna, particularly in small streams.

CONCLUSIONS

In this study, we analyzed the frequency and magnitude of stream temperature surges caused by hot runoff in watersheds of the eastern U.S. Observations from the warmer days of 2017 and 2018 indicated temperature increases of up to 10.3°C following rainfall events in the most urbanized streams. Our study is unique in that (1) we study over 100 stream temperature records covering the full range of urbanization levels and a wide array of hydrometeorological conditions, allowing a more robust statistical analysis; (2) we simultaneously study the effect of urbanization on baseline temperature and extreme temperatures following summer storms, (3) we examine a wide (although not exhaustive) range of thermal stress determinants that are selected to be relatively easy to compute based on publicly available data so that our analyses can be replicated in other watersheds. Our findings can be summarized as follows:

1. Development in the watershed (defined by low, medium, and high developed areas in the NLCD database), and percent vegetation are the best descriptors of the frequency of surges, with Spearman correlation coefficients of 0.76 and −0.77, respectively. In other words, more developed areas or ones with less green spaces are prone to more thermal surges.
2. Although this study documented a significant correlation between urbanization — defined in terms of either percent developed or impervious area — and the presence of intense temperature surges, urbanization is not the primary determinant of EMT or temperature peak after a surge. These two variables, indicating the surge

intensity, are best explained by discharge, drainage area, and air or stream temperature immediately before the surge. The average peak temperature during surge is found to be positively correlated with both the average baseline stream temperature before surges (Figure 5d, Spearman correlation $r = 0.96$) and the average daily maximum stream temperature on undisturbed days (Spearman correlation $r = 0.82$). This result indicates that warmer baseline temperatures and surges during runoff combine to increase the thermal risks in these streams.
3. These warmer stream temperatures on undisturbed days are shown to also be driven by increased development in the watershed. Comparing stream temperature extremes on disturbed days (those with at least one surge) with undisturbed baseline days (when no surges occurred) in 2017–2018, we found that already-elevated maximum temperatures were further exacerbated by the input of hot runoff in some highly developed streams.

The frequency and intensity of surges in urban watersheds, therefore, add to their warmer baseline, indicating the development of a HUHI. This phenomenon is driven by the same urban land use modification that modulates surface and air UHIs (and subsurface UHI to a lesser extent), and therefore it would be remiss not to link them and seek common mitigation measures. In addition, many of the streams we study here are located in the Chesapeake Bay watershed, which has been shown by previous studies (Ding and Elmore 2015; Rice and Jastram 2015) to be warming. This thermal pollution can therefore also have downstream impacts.

Finally, if data become available, we recommend future analyses of temperature surges in more diverse climatic zones, especially involving dry regions in the western U.S. Our results also highlight the need for advancing our understanding of freshwater ecosystems and their fauna and flora's sensitivity to acute and chronic thermal pollution; the limited available information precludes a more conclusive analysis of the impacts of temperature surges on such ecosystems at present.

DATA AVAILABILITY

Most of the data used in this study are publicly available at the USGS website (accessed June 2020, https://waterdata.usgs.gov/nwis). Additional stream temperature data collected by the University of Maryland, Baltimore County, can be downloaded from http://hiscentral.cuahsi.org.

SUPPORTING INFORMATION

Additional supporting information may be found online under the Supporting Information tab for this article: Summary of analyzed data and temperature surge statistics for each gage.

ACKNOWLEDGMENTS

This work was supported by the Army Research Office under contracts W911NF-15-1-0003 and W911NF-20-1-0216 (program Manager Julia Barzyk); the U.S. National Science Foundation through ICER 1664021, DEB 1855277, CBET1444758 (The Urban Water Innovation Network Sustainability Research Network), and CBET 1444755 (Urban Resilience to Extremes Sustainability Research Network); and Chesapeake Bay Trust Grant 15828, and the Moore Charitable Foundation's Science to Action Fund through the Princeton University School of Engineering and Applied Science. We also thank USGS for making its data available, which allowed the accomplishment of this research.

AUTHOR CONTRIBUTIONS

Einara Zahn: Conceptualization; Data curation; Formal analysis; Methodology; Writing-original draft; Writing-review & editing. **Claire Welty:** Resources; Writing-review & editing. **James Smith:** Methodology; Writing-review & editing. **Stanley Kemp:** Writing-review & editing. **Mary Lynn Baeck:** Resources; Writing-review & editing. **Elie Bou-Zeid:** Conceptualization; Funding acquisition; Methodology; Writing-original draft; Writing-review & editing.

LITERATURE CITED

Anderson, W.P., R.E. Storniolo, and J.S. Rice. 2011. "Bank Thermal Storage as a Sink of Temperature Surges in Urbanized Streams." *Journal of Hydrology* 409 (1–2): 525–37. https://doi.org/10.1016/j.jhydrol.2011.08.059.

Baruch, E.M., K.A. Voss, J.R. Blaszczak, J. Delesantro, D.L. Urban, and E.S. Bernhardt. 2018. "Not All Pavements Lead to Streams: Variation in Impervious Surface Connectivity Affects Urban Stream Ecosystems." *Freshwater Science* 37 (3): 673–84. https://doi.org/10.1086/699014.

Beitinger, T.L., and W.A. Bennett. 2000. "Quantification of the Role of Acclimation Temperature in Temperature Tolerance of Fishes." *Environmental Biology of Fishes* 58 (3): 277–88. https://doi.org/10.1023/A:1007618927527.

Booth, D.B., K.A. Kraseski, and C. Rhett Jackson. 2014. "Local-Scale and Watershed-Scale Determinants of Summertime Urban Stream Temperatures." *Hydrological Processes* 28 (4): 2427–38. https://doi.org/10.1002/hyp.9810.

Brans, K.I., J.M.T. Engelen, C. Souffreau, and L. De Meester. 2018. "Urban Hot-Tubs: Local Urbanization Has Profound

Effects on Average and Extreme Temperatures in Ponds." *Landscape and Urban Planning* 176: 22–29. https://doi.org/10.1016/j.landurbplan.2018.03.013.

Cook, M., J.R. Schott, J. Mandel, and N. Raqueno. 2014. "Development of an Operational Calibration Methodology for the Landsat Thermal Data Archive and Initial Testing of the Atmospheric Compensation Component of a Land Surface Temperature (LST) Product from the Archive." *Remote Sensing* 6 (11): 11244–66. https://doi.org/10.3390/rs61111244.

Croghan, D., A.F. Van Loon, J.P. Sadler, C. Bradley, and D.M. Hannah. 2019. "Prediction of River Temperature Surges is Dependent on Precipitation Method." *Hydrological Processes* 33 (1): 144–59. https://doi.org/10.1002/hyp.13317.

Demars, B.O.L., J. Russell Manson, J.S. Ólafsson, G.M. Gíslason, R. Gudmundsdóttir, G. Woodward, J. Reiss, D.E. Pichler, J.J. Rasmussen, and N. Friberg. 2011. "Temperature and the Metabolic Balance of Streams." *Freshwater Biology* 56 (6): 1106–21. https://doi.org/10.1111/j.1365-2427.2010.02554.x.

Ding, H., and A.J. Elmore. 2015. "Spatio-Temporal Patterns in Water Surface Temperature from Landsat Time Series Data in the Chesapeake Bay, U.S.A." *Remote Sensing of Environment* 168: 335–48. https://doi.org/10.1016/j.rse.2015.07.009.

Egorov, A., D. Roy, H. Zhang, Z. Li, L. Yan, and H. Huang. 2019. "Landsat 4, 5 and 7 (1982 to 2017) Analysis Ready Data (ARD) Observation Coverage over the Conterminous United States and Implications for Terrestrial Monitoring." *Remote Sensing* 11. https://doi.org/10.3390/rs11040447.

Fanelli, R.M., K.L. Prestegaard, and M.A. Palmer. 2019. "Urban Legacies: Aquatic Stressors and Low Aquatic Biodiversity Persist Despite Implementation of Regenerative Stormwater Conveyance Systems." *Freshwater Science* 38 (4): 818–33. https://doi.org/10.1086/706072.

Gu, C., W.P. Anderson Jr, J.D. Colby, and C.L. Coffey. 2015. "Air-Stream Temperature Correlation in Forested and Urban Headwater Streams in the Southern Appalachians." *Hydrological Processes* 29 (6): 1110–18. https://doi.org/10.1002/hyp.10225.

Hannah, D.M., and G. Garner. 2015. "River Water Temperature in the United Kingdom: Changes over the 20th Century and Possible Changes over the 21st Century." *Progress in Physical Geography: Earth and Environment* 39 (1): 68–92. https://doi.org/10.1177/0309133314550669.

Hathaway, J.M., R.J. Winston, R.A. Brown, W.F. Hunt, and D.T. McCarthy. 2016. "Temperature Dynamics of Stormwater Runoff in Australia and the USA." *Science of the Total Environment* 559: 141–50. https://doi.org/10.1016/j.scitotenv.2016.03.155.

Herb, W.R., B. Janke, O. Mohseni, and H.G. Stefan. 2008. "Thermal Pollution of Streams by Runoff from Paved Surfaces." *Hydrological Processes* 22 (7): 987–99. https://doi.org/10.1002/hyp.6986.

Herb, W.R., B. Janke, O. Mohseni, and H.G. Stefan. 2009. "Runoff Temperature Model for Paved Surfaces." *Journal of Hydrologic Engineering* 14 (10): 1146–55. https://doi.org/10.1061/(ASCE)HE.1943-5584.0000108.

Hester, E.T., and K.S. Bauman. 2013. "Stream and Retention Pond Thermal Response to Heated Summer Runoff from Urban Impervious Surfaces." *Journal of the American Water Resources Association* 49 (2): 328–42. https://doi.org/10.1111/jawr.12019.

Hirsch, R.M., and L.A. De Cicco. 2015. "User Guide to Exploration and Graphics for RivEr Trends (EGRET) and Data Retrieval: R Packages for Hydrologic Data (Version 2.0, February 2015)." U.S. Geological Survey Techniques and Methods Book 4, Chap. A10. ss.

Hofmeister, K.L., C.M. Cianfrani, and W. Cully Hession. 2015. "Complexities in the Stream Temperature Regime of a Small Mixed-Use Watershed, Blacksburg, VA." *Ecological Engineering* 78: 101–11. https://doi.org/10.1016/j.ecoleng.2014.05.019.

Homer, C., J. Dewitz, S. Jin, G. Xian, C. Costello, P. Danielson, L. Gass *et al*. 2020. "Conterminous United States Land Cover Change Patterns 2001–2016 from the 2016 National Land Cover Database." *ISPRS Journal of Photogrammetry and Remote Sensing* 162: 184–99. https://doi.org/10.1016/j.isprsjprs.2020.02.019.

Iezzi, F., and M.T. Todisco. 2015. "Stream Temperature Estimated In Situ from Thermal-Infrared Images: Best Estimate and Uncertainty." *Journal of Physics: Conference Series* 655 (November): 012063. https://doi.org/10.1088/1742-6596/655/1/012063.

Janke, B.D., W.R. Herb, O. Mohseni, and H.G. Stefan. 2009. "Simulation of Heat Export by Rainfall–Runoff from a Paved Surface." *Journal of Hydrology* 365 (3–4): 195–212. https://doi.org/10.1016/j.jhydrol.2008.11.019.

Kaushal, S.S., A.J. Gold, S. Bernal, T.A.N. Johnson, K. Addy, A. Burgin, D.A. Burns *et al*. 2018. "Watershed 'Chemical Cocktails': Forming Novel Elemental Combinations in Anthropocene Fresh Waters." *Biogeochemistry* 141 (3): 281–305. https://doi.org/10.1007/s10533-018-0502-6.

Kemp, S. 2014. "The Potential and Limitations of Linking Biological Monitoring Data and Restoration Needs of Urbanized Waterways: A Case Study." *Environmental Monitoring and Assessment* 186 (6): 3859–73. https://doi.org/10.1007/s10661-014-3663-3.

Ketabchy, M., D.J. Sample, T. Wynn-Thompson, and M.N. Yazdi. 2019. "Simulation of Watershed-Scale Practices for Mitigating Stream Thermal Pollution Due to Urbanization." *Science of the Total Environment* 671: 215–31. https://doi.org/10.1016/j.scitotenv.2019.03.248.

Kowalski, K.T., J.P. Schubauer, C.L. Scott, and J.R. Spotila. 1978. "Interspecific and Seasonal Differences in the Temperature Tolerance of Stream Fish." *Journal of Thermal Biology* 3 (3): 105–08. https://doi.org/10.1016/0306-4565(78)90001-3.

Krause, C.W., B. Lockard, T.J. Newcomb, D. Kibler, V. Lohani, and D.J. Orth. 2004. "Predicting Influences of Urban Development on Thermal Habitat in a Warm Water Stream." *Journal of the American Water Resources Association* 40 (6): 1645–58. https://doi.org/10.1111/j.1752-1688.2004.tb01612.x.

LeBlanc, R.T., R.D. Brown, and J.E. FitzGibbon. 1997. "Modeling the Effects of Land Use Change on the Water Temperature in Unregulated Urban Streams." *Journal of Environmental Management* 49 (4): 445–69. https://doi.org/10.1006/jema.1996.0106.

Leopold, L.B. 1968. "Hydrology for Urban Land Planning: A Guidebook on the Hydrologic Effects of Urban Land Use." Circular 554. U.S. Geological Survey. https://pubs.er.usgs.gov/publication/cir554.

Li, D., and E. Bou-Zeid. 2013. "Synergistic Interactions between Urban Heat Islands and Heat Waves: The Impact in Cities Is Larger than the Sum of Its Parts." *Journal of Applied Meteorology and Climatology* 52 (9): 2051–64. https://doi.org/10.1175/JAMC-D-13-02.1.

Li, H., J.T. Harvey, T.J. Holland, and M. Kayhanian. 2013. "The Use of Reflective and Permeable Pavements as a Potential Practice for Heat Island Mitigation and Stormwater Management." *Environmental Research Letters* 8 (1): 015023. https://doi.org/10.1088/1748-9326/8/1/015023.

Manoli, G., S. Fatichi, M. Schläpfer, K. Yu, T.W. Crowther, N. Meili, P. Burlando, G.G. Katul, and E. Bou-Zeid. 2019. "Magnitude of Urban Heat Islands Largely Explained by Climate and Population." *Nature* 573 (7772): 55–60. https://doi.org/10.1038/s41586-019-1512-9.

Menberg, K., P. Bayer, K. Zosseder, S. Rumohr, and P. Blum. 2013. "Subsurface Urban Heat Islands in German Cities." *Science of the Total Environment* 442: 123–33. https://doi.org/10.1016/j.scitotenv.2012.10.043.

Mohajerani, A., J. Bakaric, and T. Jeffrey-Bailey. 2017. "The Urban Heat Island Effect, Its Causes, and Mitigation, with Reference to the Thermal Properties of Asphalt Concrete." *Journal of Environmental Management* 197: 522–38. https://doi.org/10.1016/j.jenvman.2017.03.095.

Nelson, K.C., and M.A. Palmer. 2007. “Stream Temperature Surges under Urbanization and Climate Change: Data, Models, and Responses.” *Journal of the American Water Resources Association* 43 (2): 440–52. https://doi.org/10.1111/j.1752-16882007.00034.x.

Oke, T.R. 1982. “The Energetic Basis of the Urban Heat Island.” *Quarterly Journal of the Royal Meteorological Society* 108 (455): 1–24. https://doi.org/10.1002/qj.49710845502.

Oke, T.R. 1995. “The Heat Island of the Urban Boundary Layer: Characteristics, Causes and Effects.” In *Wind Climate in Cities. NATO ASI Series (Series E: Applied Sciences)* (Volume 277), edited by J.E. Cermak, A.G. Davenport, E.J. Plate, and D.X. Viegas. Dordrecht: Springer. https://doi.org/10.1007/978-94-017-3686-2_5.

Oke, T.R., G. Mills, A. Christen, and J.A. Voogt. 2017. *Urban Climates*. Cambridge University Press. https://doi.org/10.1017/9781139016476.

Omidvar, H., E. Bou-Zeid, and M. Chiaramonte. 2019. “Physical Determinants and Reduced Models of the Rapid Cooling of Urban Surfaces during Rainfall.” *Journal of Advances in Modeling Earth Systems* 11 (5): 1364–80. https://doi.org/10.1029/2018MS001528.

Omidvar, H., J. Song, J. Yang, G. Arwatz, Z.-H. Wang, M. Hultmark, K. Kaloush, and E. Bou-Zeid. 2018. “Rapid Modification of Urban Land Surface Temperature during Rainfall.” *Water Resources Research* 54 (7): 4245–64. https://doi.org/10.1029/2017WR022241.

Peel, M.C., B.L. Finlayson, and T.A. McMahon. 2007. “Updated World Map of the Köppen-Geiger Climate Classification.” *Hydrology and Earth System Sciences* 11 (5): 1633–44. https://doi.org/10.5194/hess-11-1633-2007.

Picksley, W., and A. Deletic. 1999. “The Thermal Enrichment of Storm Runoff from Paved Areas — A Statistical Analysis.” *Journal of Water Management Modeling*. https://doi.org/10.14796/JWMM.R204-07.

Pluhowski, E.J. 1970. “Urbanization and its effect on the temperature of the streams on Long Island, New York.” Report 627D. U.S. Geological Survey. http://pubs.er.usgs.gov/publication/pp627D.

Ramamurthy, P., E. Bou-Zeid, J.A. Smith, Z. Wang, M.L. Baeck, N.Z. Saliendra, J.L. Hom, and C. Welty. 2014. “Influence of Subfacet Heterogeneity and Material Properties on the Urban Surface Energy Budget.” *Journal of Applied Meteorology and Climatology* 53 (9): 2114–29. https://doi.org/10.1175/JAMC-D-13-0286.1.

Reza, A., and T. Endreny. 2019. “A River Temperature Model to Assist Managers in Identifying Thermal Pollution Causes and Solutions.” *Water* 11 (5): 1060. https://doi.org/10.3390/w11051060.

Reza, A., T. Endreny, and D. Nowak. 2020. “A Model to Integrate Urban River Thermal Cooling in River Restoration.” *Journal of Environmental Management* 258. https://doi.org/10.1016/j.jenvman.2019.110023.

Rice, Jr., J.S., W.P. Anderson, and C.S. Thaxton. 2011. “Urbanization Influences on Stream Temperature Behavior within Low-Discharge Headwater Streams.” *Hydrological Research Letters* 5: 27–31. https://doi.org/10.3178/hrl.5.27.

Rice, K.C., and J.D. Jastram. 2015. “Rising Air and Stream-Water Temperatures in Chesapeake Bay Region, USA.” *Climatic Change* 128 (1): 127–38.

Rossi, L., and R.E. Hari. 2007. “Screening Procedure to Assess the Impact of Urban Stormwater Temperature to Populations of Brown Trout in Receiving Water.” *Integrated Environmental Assessment and Management* 3 (3): 383–92. https://doi.org/10.1002/ieam.5630030309.

Sailor, D.J., M. Georgescu, J.M. Milne, and M.A. Hart. 2015. “Development of a National Anthropogenic Heating Database with an Extrapolation for International Cities.” *Atmospheric Environment* 118: 7–18. https://doi.org/10.1016/j.atmosenv.2015.07.016.

Santamouris, M. 2011. “Heat-Island Effect.” In *Chap. 5: Energy and Climate in the Urban Built Environment*, edited by M. Santamouris, 48–66. New York: Routledge.

Scrine, J., M. Jochum, J.S. Ólafsson, and E.J. O’Gorman. 2017. “Interactive Effects of Temperature and Habitat Complexity on Freshwater Communities.” *Ecology and Evolution* 7 (22): 9333–46. https://doi.org/10.1002/ece3.3412.

Somers, K.A., E.S. Bernhardt, J.B. Grace, B.A. Hassett, E.B. Sudduth, S. Wang, and D.L. Urban. 2013. “Streams in the Urban Heat Island: Spatial and Temporal Variability in Temperature.” *Freshwater Science* 32 (1): 309–26. https://doi.org/10.1899/12-046.1.

Somers, K.A., E.S. Bernhardt, B.L. McGlynn, and D.L. Urban. 2016. “Down-Stream Dissipation of Storm Flow Heat Pulses: A Case Study and Its Landscape-Level Implications.” *Journal of the American Water Resources Association* 52 (2): 281–97. https://doi.org/10.1111/1752-1688.12382.

Stull, R. 2011. “Wet-Bulb Temperature from Relative Humidity and Air Temperature.” *Journal of Applied Meteorology and Climatology* 50 (11): 2267–69. https://doi.org/10.1175/JAMC-D-11-0143.1.

Sun, N., J. Yearsley, N. Voisin, and D.P. Lettenmaier. 2015. “A Spatially Distributed Model for the Assessment of Land Use Impacts on Stream Temperature in Small Urban Watersheds.” *Hydrological Processes* 29 (10): 2331–45. https://doi.org/10.1002/hyp.10363.

Terpin, K.M., J.R. Spotila, and R.R. Koons. 1976. “Effect of Photoperiod on the Temperature Tolerance of the Blacknose Dace, *Rhinichthys atratulus*.” *Comparative Biochemistry and Physiology Part A: Physiology* 53 (3): 241–44. https://doi.org/10.1016/S0300-9629(76)80028-X.

Thompson, A.M., T. Wilson, J.M. Norman, A.L. Gemechu, and A. Roa-Espinosa. 2008. “Modeling the Effect of Summertime Heating on Urban Runoff Temperatures.” *Journal of the American Water Resources Association* 44 (6): 1548–63. https://doi.org/10.1111/j.1752-1688.2008.00259.x.

Walsh, C.J., A.H. Roy, J.W. Feminella, P.D. Cottingham, P.M. Groffman, and R.P. Morgan. 2005. “The Urban Stream Syndrome: Current Knowledge and the Search for a Cure.” *Journal of the North American Benthological Society* 24 (3): 706–23. https://doi.org/10.1899/04-028.1.

Welty, C., and J.T. Kemper. 2019. *UMBC Water Quality Observations, 2010–Present*. Baltimore, MD: University of Maryland, Baltimore County, Center for Urban Environmental Research and Education. http://hiscentral.cuahsi.org.

Westaway, R., and P.L. Younger. 2016. “Unravelling the Relative Contributions of Climate Change and Ground Disturbance to Subsurface Temperature Perturbations: Case Studies from Tyneside, UK.” *Geothermics* 64: 490–515. https://doi.org/10.1016/j.geothermics.2016.06.009.

Yang, J., and E. Bou-Zeid. 2018. “Should Cities Embrace Their Heat Islands as Shields from Extreme Cold?” *Journal of Applied Meteorology and Climatology* 57 (6): 1309–20. https://doi.org/10.1175/JAMC-D-17-0265.1.

Yang, L., C. Huang, C.G. Homer, B.K. Wylie, and M.J. Coan. 2003. “An Approach for Mapping Large-Area Impervious Surfaces: Synergistic Use of Landsat-7 ETM+ and High Spatial Resolution Imagery.” *Canadian Journal of Remote Sensing* 29 (2): 230–40. https://doi.org/10.5589/m02-098.

Zeiger, S.J., and J.A. Hubbart. 2015. “Urban Stormwater Temperature Surges: A Central US Watershed Study.” *Hydrology* 2 (4): 193–209. https://doi.org/10.3390/hydrology2040193.